

## REPORT DOCUMENTATION PAGE

Form Approved  
OMB No. 0704-0188

2

AD-A275 628



is estimated to average 1 hour per response, including the time for reviewing instructions, searching existing data sources, gathering and reviewing the collection of information. Send comments regarding this burden estimate or any other aspect of this collection of information, including suggestions for reducing this burden, to Washington Headquarters Services, Directorate for Information Operations and Reports, 1215 Jefferson Avenue, Alexandria, VA 22304-6146. Paperwork Reduction Project (0704-0188), Washington, DC 20503.

REPORT DATE

3. REPORT TYPE AND DATES COVERED

Reprint September 1991 - September 1993

## 4. TITLE AND SUBTITLE

Post-Perforation Characteristics of Yawed Long Rods

## 5. FUNDING NUMBERS

DAAL03-91-C-0021

## 6. AUTHOR(S)

A. J. Piekutowski and C. E. Anderson, Jr.

## 7. PERFORMING ORGANIZATION NAME(S) AND ADDRESS(ES)

Southwest Research Institute Univ. of Dayton Res. Inst.  
6220 Culebra Road 300 College Park  
San Antonio, TX 78228-0510 Dayton, OH 45469-0182

8. PERFORMING ORGANIZATION  
REPORT NUMBER

## 9. SPONSORING/MONITORING AGENCY NAME(S) AND ADDRESS(ES)

U. S. Army Research Office  
P. O. Box 12211  
Research Triangle Park, NC 27709-2211

SPONSORING/MONITORING  
AGENCY REPORT NUMBER

ARL 29647.2-MA

## 11. SUPPLEMENTARY NOTES

The view, opinions and/or findings contained in this report are those of the author(s) and should not be construed as an official Department of the Army position, policy, or decision, unless so designated by other documentation.

## 12a. DISTRIBUTION/AVAILABILITY STATEMENT

Approved for public release; distribution unlimited.

## 12b. DISTRIBUTION CODE

## 13. ABSTRACT (Maximum 200 words)

Perforation of finite-thickness, rolled homogeneous armor (RHA) plate by a ductile, tungsten-alloy, long-rod penetrator will reduce the length and velocity of the residual rod. Test results presented in the paper show the angle of inclination (yaw) of the rod also contributes to the reduction of residual-rod length and velocity. Two sizes of 90-percent-tungsten-alloy rods were fired at normal incidence (0° obliquity) against RHA plates with nominal impact velocities of 2.2 km/s. Multiple-exposure, orthogonal-pair flash radiographs were used to obtain pre-impact pitch and yaw of the rods and residual-rod length, velocity, and trajectory data. In addition to erosion, two post-impact mechanisms were observed to reduce the length and velocity of the yawed rod--(1) extremely localized bending and fracture of the front of the rod and (2) a second collision of the rod with the penetration channel sidewall.

94 2 08 03 1

94-04303



11 pg

## 14. SUBJECT TERMS

long-rod penetration, perforation, RHA, yawed impact

## 15. NUMBER OF PAGES

## 16. PRICE CODE

17. SECURITY CLASSIFICATION  
OF REPORT

UNCLASSIFIED

18. SECURITY CLASSIFICATION  
OF THIS PAGE

UNCLASSIFIED

19. SECURITY CLASSIFICATION  
OF ABSTRACT

UNCLASSIFIED

## 20. LIMITATION OF ABSTRACT

UL



## EXPERIMENTAL PROCEDURE

The tests described in this paper were performed in the Impact Physics Laboratory of the University of Dayton Research Institute. Long tungsten rods, with length-to-diameter ratios ( $L/D$ ) of 20, were fired at normal incidence into finite-thickness plates of rolled homogeneous armor (RHA) using a 50/20 mm, two-stage, light-gas gun. A total of 14 tests with a nominal impact velocity of 2.20 km/s were performed. The rods used in these tests were identical to rods used in a series of tests to evaluate scale modeling issues in armor penetration experiments [6]. In that series of tests, 1/3.15-, 1/6.30-, and 1/12.60-scale long rods were fired into several types of targets.

Puller-type sabots were required to successfully launch the 1/3.15- and 1/6.30-scale rods to the desired velocity of 2.20 km/s. A portion of the surface of the rod and the bore of the sabot were fabricated with machine-screw threads to facilitate transfer of launch loads between the rod and the sabot. Although not necessary for launch purposes, a short threaded section was incorporated in the design of the 1/12.60-scale rod to preserve similarity of the rod designs. A 1/6.30- and 1/12.60-scale rod are shown, with appropriate details, in Fig. 1. The rods were made from WN008F, a tungsten alloy consisting of 90 percent tungsten, 8 percent nickel, and 2 percent iron ( $\rho = 17.13 \text{ g/cm}^3$ ). A hollowed-out, light-weight aluminum flare was lightly pressed on the end of the rod. Nominal rod/flare weights for the 1/6.30- and 1/12.60-scale rods were 19.1/0.40 g and 2.36/0.10 g, respectively.

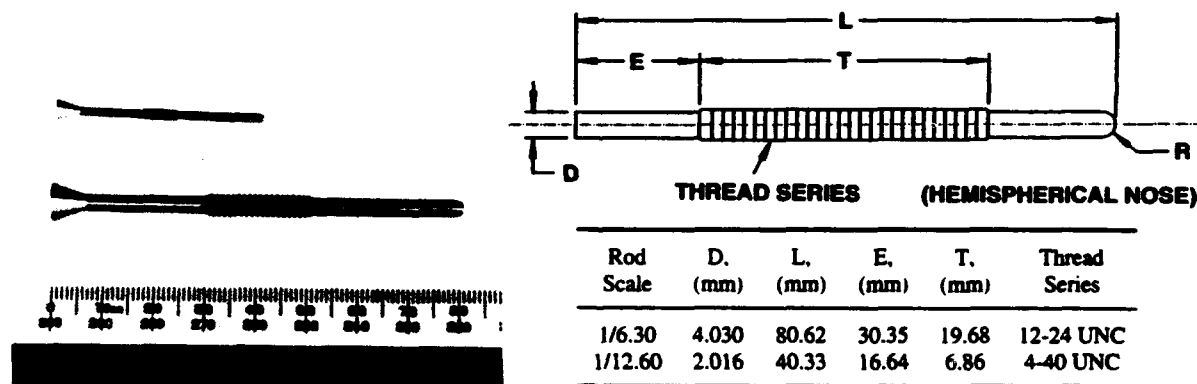


Fig. 1. Long-rod penetrators used in tests.

The targets used with the 1/12.60-scale rods were 2.5-cm-thick by 10.2-cm-square plates of RHA with a nominal hardness of  $R_C 30$ . Heat-treated, A.I.S.I 4340 alloy-steel plates, 5.1-cm-thick by 10.2-cm-square, were used as targets for the 1/6.30-scale rods. The target plates were clamped in a test fixture mounted inside the target chamber of the range.

Three pairs of orthogonal flash x-rays were used to preview the impact and emergence of the residual rod. The relationship of the target, x-ray sources, and other relevant articles used to produce one of the orthogonal views is shown in Fig. 2. Firing of the x-rays at predetermined time intervals was accomplished with use of time-delay generators. An event-initiating trigger pulse was generated when the rod passed through a laser-photodetector system located a short distance uprange of the target. Firing of the first pair of x-rays produced the pre-impact views of the rod. Fiducial pins, extending into the field of view of both x-ray heads,

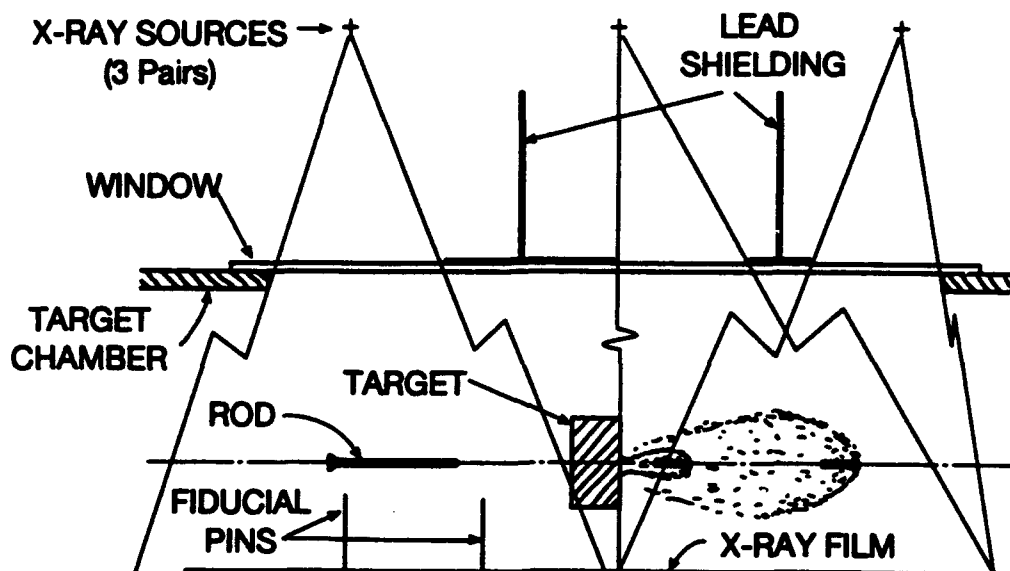


Fig. 2. Setup used to obtain multiple-exposure, orthogonal-pair flash radiographs.

provided the reference for measurement of pitch and yaw of the rod. The second and third pair of x-rays were used to produce a double-exposed image of the residual rod and the associated debris. Careful positioning of the x-ray sources with respect to the range center line, target, and film facilitated determination of the trajectory of the residual rod. The residual velocity of the rod remnant was computed using the displacement of the residual rod and the measured time between firing of the x-rays. Residual-rod length and trajectory were also determined from the radiographs.

## RESULTS

Radiographs of four tests using 1/12.60-scale rods, at varying angles of inclination, are presented in Fig. 3. Only a top or a side view is provided for each test. As shown in Fig. 3, the length of the residual rod decreased significantly as the angle of inclination increased. The inclination angle of the rod at impact was determined using pitch and yaw measurements taken from the x-rays. Pitch, in this paper, is the upward or downward inclination of the rod as observed in the side-view radiograph. Yaw is the inclination of the rod to the right or left as seen in the top-view radiograph. The inclination of the rod was determined to be the square root of the sum of the squares of the pitch and yaw angles of the rod.

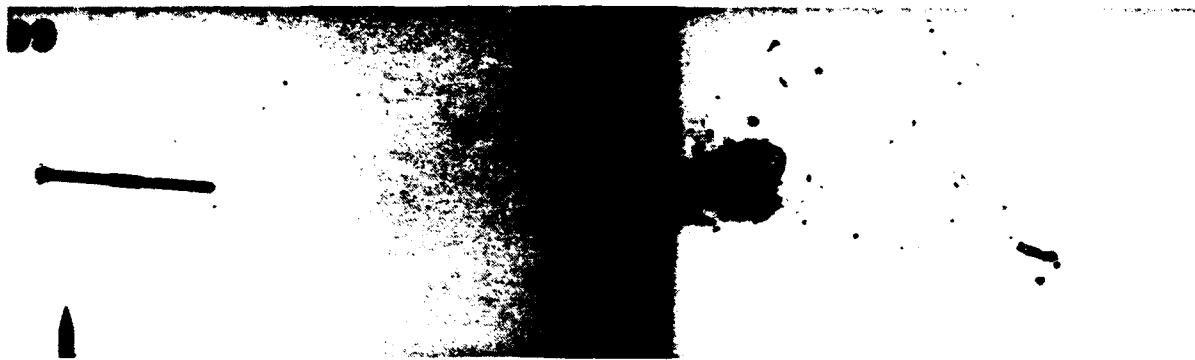
The radiographs from the 14 tests were also analyzed to determine the length,  $L_r$ , trajectory, and velocity,  $V_r$ , of the residual-rod fragment(s). Results of the analyses are presented in the table with other pertinent test data. The length of the residual rod reported in the table was the length of the longest piece of the rod seen in the debris cloud. In most instances, this piece was at the front of the debris cloud. In a majority of the tests, the rear end of the residual rod was broken as shown in the radiograph from Shot 4-1498 in Fig. 3.



Shot 4-1498

Inclination = 3.7 Degrees

$V_s = 2.21 \text{ km/s}$



Shot 4-1499

Inclination = 4.6 Degrees

$V_s = 2.17 \text{ km/s}$



Shot 4-1496

Inclination = 7.2 Degrees

$V_s = 2.25 \text{ km/s}$



Shot 4-1495

Inclination = 16.9 Degrees

$V_s = 2.17 \text{ km/s}$

Fig. 3. Radiographs of four tests employing 1/12.60-scale long rods with varying angles of inclination.

## Residual Rod Data

Shot No.	Hardness (R <sub>C</sub> )	V <sub>S</sub> (km/s)	Inclination (Degrees)	V <sub>r</sub> (km/s)	V <sub>r</sub> /V <sub>S</sub> (---)	L <sub>r</sub> (cm)	L <sub>r</sub> /L <sub>0</sub> (---)	Azimuth (deg) Pre-Impact      Residual	
1 / 12.60 Scale Rods - L <sub>0</sub> = 4.03 cm									
4-1495	33	2.17	16.9	Did Not Penetrate				7	---
4-1496	33	2.25	7.2	1.76	0.782	0.51	0.126	336	337
4-1497	28	2.18	4.3	1.90	0.872	0.79	0.195	282	293
4-1498	30	2.21	3.7	2.02	0.914	1.73	0.428	214	214
4-1499	30	2.17	4.6	1.94	0.894	0.91	0.226	9	8
4-1530	28	2.18	5.2	1.91	0.876	0.71	0.176	51	52
4-1531	29	2.16	5.3	1.74	0.806	0.58	0.145	337	326
4-1532	32	2.18	5.2	1.80	0.826	0.61	0.151	358	346
4-1535	32	2.19	7.6	1.61	0.735	0.40	0.100	314	311
4-1624	31	1.98	2.7	1.85	0.934	1.24	0.308	0	0
4-1652	41	2.13	10.8	1.02	0.479	Small Fragments		199	---
1 / 6.30 Scale Rods - L <sub>0</sub> = 8.06 cm									
4-1623	30	2.22	4.6	2.09	0.941	1.96	0.242	276	280
4-1626	31	2.24	10.9	1.57	0.700	1.30*	0.161	198	206
4-1651	32	2.18	8.9	1.86	0.853	0.94	0.116	202	206

\* Y-shaped and split open.

## DISCUSSION

Residual rod lengths and velocities were normalized by dividing them by the initial rod length, L<sub>0</sub>, and impact velocity, V<sub>S</sub>. Normalized rod length and velocity are shown as a function of the inclination angle of the rod at impact in Fig. 4. Silsby *et al.* [5] have given an expression for determination of a critical yaw (inclination) angle, i.e., the angle at which the tail of a long-rod penetrator will touch the side wall of a crater. The expression is as follows:

$$\gamma_{cr} = \sin^{-1} [(H-D) / 2L].$$

In this expression, D and L are the rod diameter and length, respectively, and H is the diameter of the penetration channel. At an impact velocity of 2.20 km/s,  $H \cong 2D$  for work described in this paper. For an L/D = 20 rod traveling at 2.20 km/s, the critical angle, as defined above, is about 1.5 degrees. Inclination angles for all the tests in this paper were considerably larger than the critical yaw angle defined by Silsby *et al.* Examination of the radiographs for the tests presented in this paper showed that the tail end of the residual rod was broken or at least severely deformed for all tests. Clearly, significant interference between the rod end and the sidewall of the penetration channel had occurred at some point in the penetration process. In the scale modeling series [6], a 1/12.60-scale rod travelling at 2.21 km/s impacted a 3.89-cm-thick, 4340 alloy-steel target at essentially zero degree inclination. A 0.81-cm-long residual rod, was observed leaving the target. The tail end of the residual rod was intact and undamaged for this test.

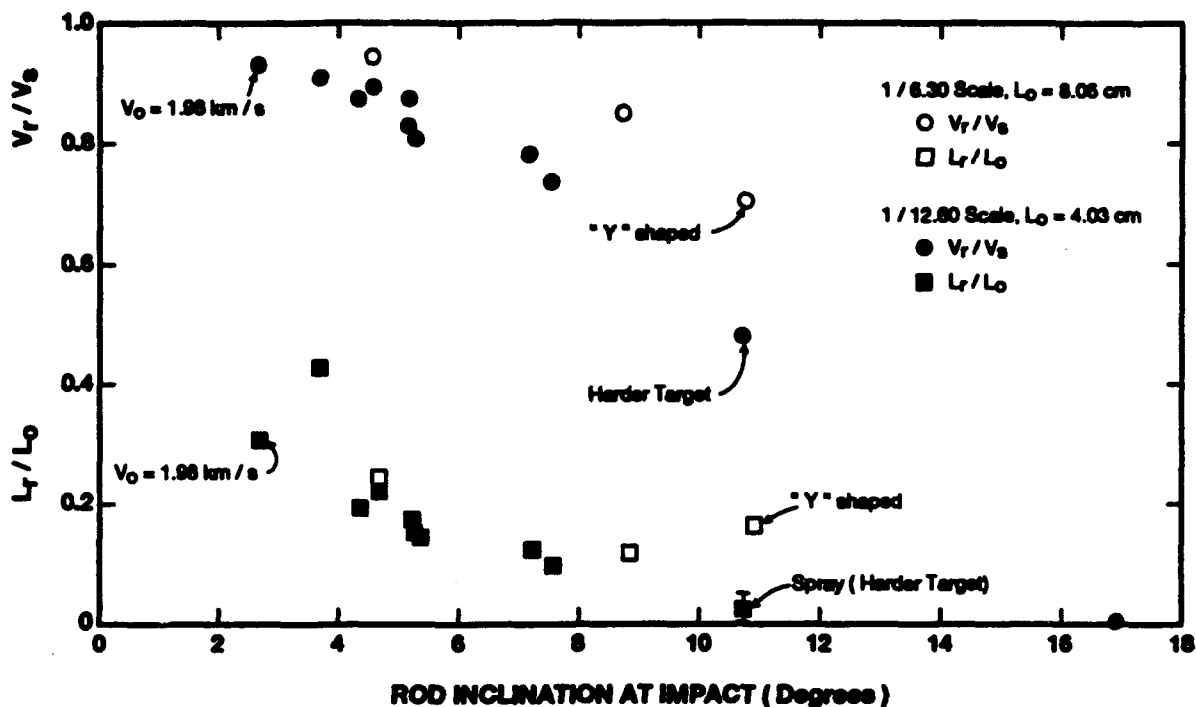


Fig. 4. Normalized-residual rod velocity and length as a function of inclination angle of rod at impact. Impact velocity,  $V_s$ , was 2.2 km/s unless noted otherwise.

In addition to the straight-line motion of the residual rod (fragment) away from the target, all fragments were observed to have a small to large angular velocity. Use of the orthogonal-pair flash x-rays allowed the trajectory of the estimated center of mass to be determined for the rotating residual-rod fragments. The azimuth of the trajectory of the fragment, when viewed from a position facing the front of the target, was compared with the azimuth of the tail of the rod before impact in Fig. 5. The agreement of the azimuth angles is remarkable. Deviation of the trajectory of the residual rod from the shot center line was also determined (but not presented in the table). Agreement of the inclination angle of the trajectory of the residual rod with the inclination angle of the rod at impact was very good. The observed change in the direction of motion of the rod fragment from the shot center line was clearly related to the inclination of the rod at impact. Understanding the kinetics of the penetration of yawed long rods remains an area for further study.

Comparison of residual-fragment data for the different rod scales showed that residual-rod lengths appeared to scale (for the limited data available). Normalized residual-rod velocities do not scale and are considerably higher for the 1/6.30-scale tests than for the 1/12.60-scale tests. Post-perforation trajectory characteristics of the rod fragments were the same for both rod scales, however.

Use of the larger scale rod provided an additional benefit since the radiographs exhibited considerably more detail in the views of the residual rod and fragments. Side and top views of that portion of the radiographs showing post-perforation performance of a 1/6.30-scale rod are presented in Fig. 6. A similar view for a 1/12.60-scale rod is also presented in Fig. 6. The yaw-plane view of the residual rod from the 1/6.30-scale test clearly shows that the nose of the rod experienced extremely localized and severe bending shortly before emerging from

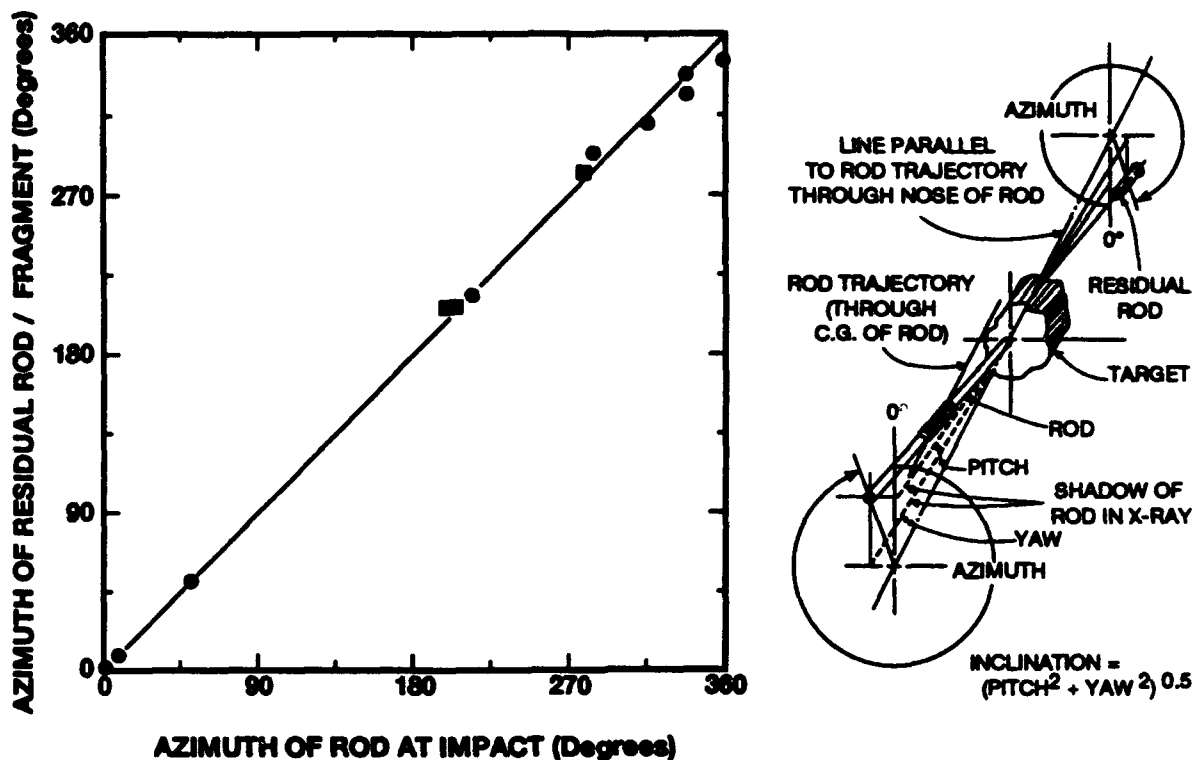


Fig. 5. Azimuth of residual rod as function of azimuth of the rod at impact.

the penetration channel. The eroding end of the rod was bent around to form a tight hook. Several fractures developed during bending. Separation of the front pieces of rod is well underway in the second view of the debris. Also evident in the second view (in the yaw plane) is a short section of threaded rod (see arrow in figure) trailing the large rod fragment.

The end of the rod was broken in two places. A short piece of rod appears to be moving away from the rotating large piece and the piece that was the end of the rod. The behavior of the various pieces gives insight into events which occurred during penetration. When the inclined rod struck the mouth of the penetration channel, a large angular velocity was imparted to the rod. A second contact between the rod (now rotating) and the mouth of the channel was violent enough to fracture the rod in two places, deforming the section that struck the penetration channel.

Exit holes for all targets in which the inclination angle was greater than 4 degrees exhibited considerable enlargement and eccentric bell-mouthing. Exit holes for targets impacted by rods at inclination angles of less than 4 degrees were round and slightly smaller in diameter than the entrance hole diameter. Two profiles of the penetration channel produced by the 1/6.30-scale rod shown in Fig. 6 were generated using measurements taken from both sides of "slices" taken parallel to the surface of the target. The reconstructed penetration channel and several views of target "slices" are presented in Fig. 7. The exaggerated (2.6X) profile clearly shows the eccentric, bell-mouthed shape of the exit hole. A titanium disc, used in the base of the sabot, struck the upper-left quadrant of the entrance hole approximately 46  $\mu$ s after the rod impacted the target. An probable entrance-hole profile is shown in Fig. 7 in an attempt to compensate for damage done by the edge-on impact of the disc.





Shot 4-1623

Pitch Plane (Side View)

0.5 Degrees Up

$V_s = 2.22 \text{ km/s}$



Shot 4-1623

Yaw Plane (Top View)

4.6 Degrees Right

$V_s = 2.22 \text{ km/s}$



Shot 4-1624

Pitch Plane (Side View)

2.7 Degrees Down

$V_s = 1.98 \text{ km/s}$

Fig. 6. Radiographs of residual rods showing bending and failure of projectiles during late stages of penetration. Upper two views for 1/6.30-scale rod. Bottom view is of 1/12.60-scale rod.

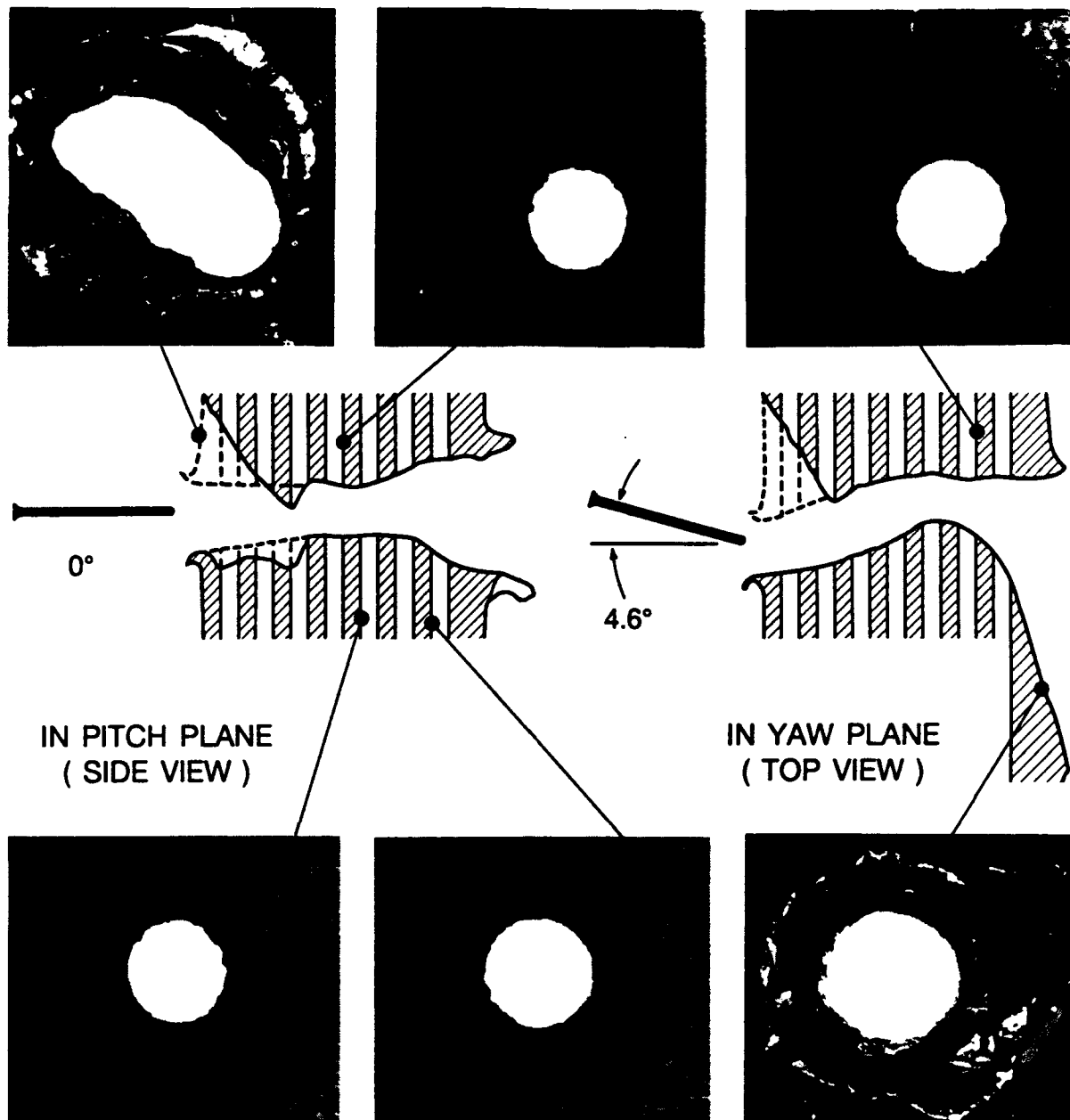


Fig. 7. Reconstruction of penetration-channel profiles in pitch and yaw planes. Data used to reconstruct profile were obtained from measurements taken from faces of target "slices". A 2.6X exaggeration of the profile was used to emphasize channel details. Channel diameter is to scale at face of fifth slice.

The shape of the residual rod observed for Shot 4-1626 was unique in the test series. A 1.3-cm-long, Y-shaped residual fragment was produced in this test. The appearance of the fragment suggested that the residual rod may have "over-rolled" a piece of rod stuck in the penetration channel, with the end result that the residual rod was flattened and split apart at the front. Some evidence of an intact but gouged tail end of the rod was observed in the radiographs.

## SUMMARY

The inclination of the rod at impact determines the inclination of the trajectory of the residual fragment. Length of the residual-rod fragment appears to scale with the scale of the rod, as a function of inclination angle of the rod. The velocity of the residual-rod fragment does not scale. Bending of the eroding end of the rod and eccentric bell-mouthing of the exit hole in the target were characteristically observed when the inclination of the rod was greater than 4 degrees.

## REFERENCES

1. C.E. Anderson, Jr., B.L. Morris, and D.L. Littlefield, "A Penetration Mechanics Database," SwRI Report 3593/001, Southwest Research Institute, San Antonio, TX, January 1992.
2. R.S. Bertke, J.F. Heyda, H.F. Swift, and M.F. Lehman, "A Study of Yawed Rod Impact," BRL CR 182, Ballistics Research Laboratory, Aberdeen Proving Ground, MD, October 1974.
3. S.J. Bless, J.P. Barber, R.S. Bertke, and H.F. Swift, "Penetration Mechanics of Yawed Rods," *Int. J. Engng. Sci.*, **16**, pp. 829-834, (1978).
4. T.W. Bjerke, G.F. Silsby, D.R. Scheffler, and R.M. Mudd, "Yawed Long-Rod Armor Penetration," *Int. J. Impact Engng*, **12**, No. 2, pp. 281-292, (1992).
5. G.F. Silsby, R.J. Roszak, and L. Giglio-Tos, "BRL's 50 mm High Pressure Powder Gun for Terminal Ballistic Testing -- The First Year's Experience," BRL-MR-03236, Ballistic Research Laboratory, Aberdeen Proving Grounds, MD, January 1983.
6. C.E. Anderson, Jr., S.A. Mullin, A.J. Piekutowski, N.W. Blaylock, and K.L. Poormon, "Scale Model Penetration Experiments: Finite-Thickness Steel Targets," in preparation.